SF2A 2011
G. Alecian, K. Belkacem, R. Samadi and D. Valls-Gabaud (eds)

THE MILKY WAY STELLAR POPULATIONS IN CFHTLS FIELDS

M. Guittet[1], M. Haywood[1] and M. Schultheis[2]

Abstract. We investigate the characteristics of the thick disk in the Canada – France – Hawaii – Telescope Legacy Survey (CFHTLS) fields, complemented at bright magnitudes with Sloan Digital Sky Survey (SDSS) data. The ([Fe/H], Z) distributions are derived in the W1 and W3 fields, and compared with simulated maps produced using the Besançon model. It is shown that the thick disk, represented in star-count models by a distinct component, is not an adequate description of the observed ([Fe/H], Z) distributions in these fields.

Keywords: the Galaxy, the thick disk, [Fe/H] abundance.

1 Introduction

Our knowledge of the characteristics of the thick disk remains limited in practically every aspects. Its structure on large scales (>kpc) is not well defined, either clumpy or smooth, and its connections with the collapsed part of the halo or the old thin disk are essentially not understood. The spectrum of possible scenarios proposed to explain its formation is still very large and really discriminant constraints are rare. The SDSS photometric survey has provided a wealth of new informations on the thick disk, see in particular Ivezić et al. (2008), Bond et al. (2010) and Lee et al. (2011). However, the data have barely been directly confronted to star-count models, and little insights have been given on how the thick disk in these models really represents the survey data. In the present work, we initiate such comparisons by comparing the Besançon model with metallicity and distance information in the W1 and W3 CFHTLS fields, and provide a brief discussion of our results.

2 Data description

Among the four fields that make the Wide Survey, W1 and W3 cover larger angular surfaces (72 and 49 square degrees) than W2 and W4 (both having 25 square degrees). They point towards higher latitudes (–61.24° and 58.39° respectively) and are consequently less affected by dust extinction, and contain a larger relative proportion of thick disk stars. We will therefore focus on W1 and W3. CFHTLS photometry starts at a substantially fainter magnitude than the SDSS, missing a large part of the thick disk. We complemented the CFHTLS catalogue at the bright end with stars from the SDSS not present in the CFHTLS fields. In the final catalogues, W1 contains $\sim$ 139 000 stars, with 16% from the SDSS, while $\sim$ 132 000 stars are found in W3 field, with 31% coming from the Sloan.
W1 and W3 are at large distances above the galactic plane. The dust extinction is very small at these latitudes. For example the Schlegel map (Schlegel et al. 1998) estimates for W1 an absorption coefficient Av of 0.087 while Jones et al. (2011) give Av=0.113. The extinction models of Arenou et al. (1992) or Hakkila et al. (1997) estimate Av values to 0.1 and 0.054 respectively. We briefly discuss the effect of extinction on distance determination and metallicities in 4.1.

[1] GEPI, Observatoire de Paris, CNRS, Université Paris Diderot; 5 Place Jules Janssen, 92190 Meudon, France
[2] Observatoire de Besançon; 41 bis, avenue de l'Observatoire, 25000 Besançon, France

3 Comparisons between the Besançon model and CFHTLS/SDSS data: Hess diagrams

3.1 The Besançon model

Simulations were made using the Besançon model (Robin et al. (2003), Haywood et al. (1997), Bienayme et al. (1987)) online version. The model includes four populations: the bulge, the thin disk, the thick disk and the halo. The metallicities of the thick disk and the halo in the online version of the model (–0.78 and –1.78 dex respectively) were shifted (to –0.6 dex and -1.5 dex) to comply with more generally accepted values, and in particular with values derived from the Sloan data (see Lee et al. (2011), who shows that the thick disk have a metallicity [Fe/H] = –0.6 dex roughly independent of vertical distances, and (Ivezić et al. (2008), Bond et al. (2010), Sesar et al. (2011), Carollo et al. (2010) or de Jong et al. (2010) for the inner halo metallicity, estimated to be about –1.5 dex). The thick disk has a scale height of 800 pc and a local stellar density ρ_0 of 6.8 % of the local thin disk, while the stellar halo is described by a power law with a flattening and a local density of 0.6%. Simulations where made assuming photometric errors as described in the SDSS.

3.2 Hess diagrams

The distributions of CFHTLS/SDSS and model stars in the g versus u–g color magnitude diagram (CMD) are shown in Fig. 1. For both diagrams, faint blue stars (u–g $\sim$ 0.9, g>18) are clearly discernible and correspond to the galactic halo. The concentration of stars at g<18, u–g $\sim$1.1, corresponds to disk stars and in particular thick disk stars. Because of the SDSS saturation at g=14 which does not allow to have a representative sample of thin disk stars, our data sample is mainly composed of thick disk and halo stars. The Besançon model shows a distinct separation between thin disk stars (u–g$\sim$1.3, g<14-15) and thick disk stars (u–g$\sim$1.1, 15<g<18) which cannot be check with the present data.

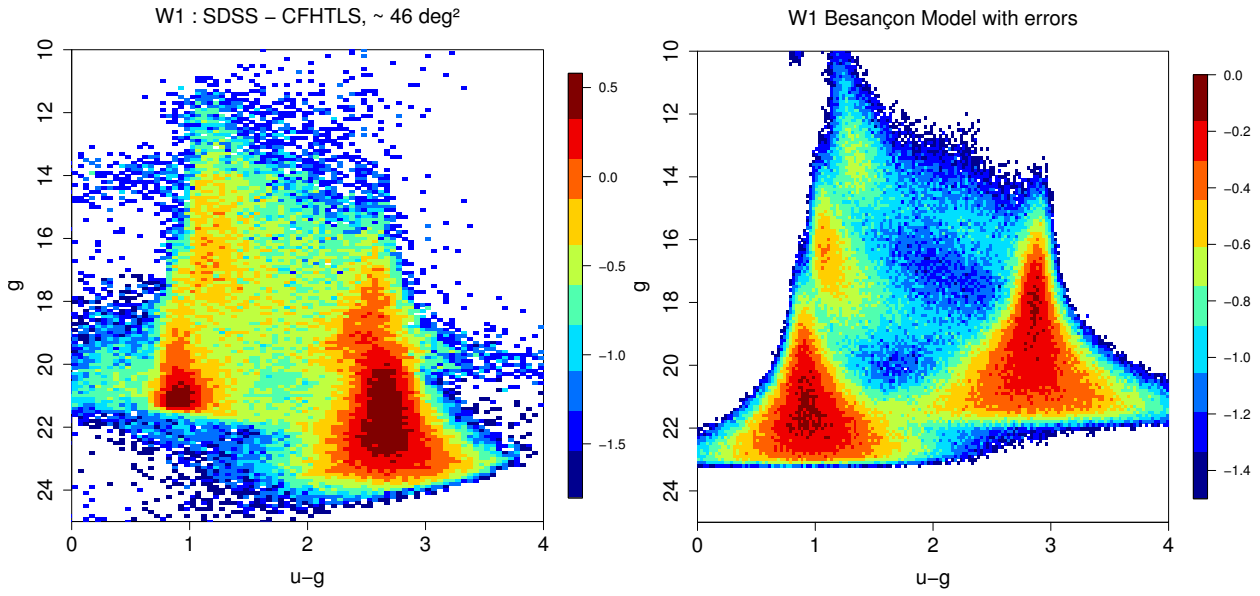

Fig. 1. Left: CFHTLS/SDSS u–g Hess diagram in W1 field. **Right:** The same as the left graphic but for the Besançon model stars to which observational errors from SDSS data have been added. The successive ridge lines due to the thin disk, thick disk and the halo main sequence stars are clearly distinguishable between 0.7<u-g<1.5.

4 Comparisons between the Besançon model and CFHTLS/SDSS data: ([Fe/H], Z) distributions

4.1 Metallicity and photometric distance determinations

Jurić et al. (2008) and Ivezić et al. (2008) have published calibrations of the metallicity and photometric parallax as a function of ugri magnitudes. The metallicity calibration has been revised in Bond et al. (2010) :

$$[\mathrm{Fe/H}] \quad = \quad \mathrm{A} + \mathrm{Bx} + \mathrm{Cy} + \mathrm{Dxy} + \mathrm{Ex}^2 + \mathrm{Fy}^2 + \mathrm{Gx}^2\mathrm{y} + \mathrm{Hxy}^2 + \mathrm{Ix}^3 + \mathrm{Jy}^3 \tag{4.1}$$

where x = $u-g$, y = $g-r$ and (A–J) = (–13.13, 14.09, 28.04, –5.51, –5.90, –58.58, 9.14, –20.61, 0.0, 58.20). This relation has been determined for F and G stars and is consequently applicable in the range : $0.2 < g-r < 0.6$ and $-0.25 + 0.5(u-g) < g-r < 0.05 + 0.5(u-g)$. This calibration only extends to –0.2 dex. Observed vertical distances Z have been calculated using $Z = \mathrm{D}\sin(\mathrm{b})$, b being the latitude of the star. Photometric distances D, such as $m_r - M_r = 5\ log(D) - 5$, were determined using the absolute magnitude calibration of Ivezić et al. (2008) which depends on the metallicity and on $g-i$ colors.

For the highest extinction values given by Jones et al. (2011), the impact on metallicities, as can be estimated using Eq. 4.1 and the absolute magnitude relation of Ivezić et al. (2008) are at most of 0.15 dex near g–r=0.5 at solar metallicities and 0.1 dex at [Fe/H]= –1 dex. Distances will be affected at most by about 20% at solar metallicities and 15% at [Fe/H]= –1 dex at g–r near 0.40-0.45.

4.2 ([Fe/H], Z) distributions

We generated catalogues with the model in the direction of W1 and W3, deriving the Z height above the plane from simulated distances and metallicities from the assumed metallicity distributions of each population. In Fig. 2 we present ([Fe/H], Z) distributions for both the data and the model. The dotted line is the median metallicity per bin of 0.5 kpc. The continuous line is the median metallicity for disk stars as shown by Bond et al. (2010) and follows rather well the disk distribution in our data. We find similar results as Bond et al. (2010) : the halo dominates the star counts above 3 kpc with a mean metallicity of about –1.5 dex. Sesar et al. (2011) studied the four CFHTLS Wide fields but with magnitudes corrected for ISM extinction. They found the mean halo metallicity in the range between –1.4 and –1.6 dex. Our estimate of the extinction effect would shift metallicities to about 0.15 dex at most, and shows that our mean halo metallicity is in good agreement with their estimates.

The interesting point worth of notice is the conspicuous, distinct, pattern that represents the thick disk in the model and which clearly is absent in the data. As expected, the standard thick disk model dominates the counts between 1 and 4 kpc, while in the data, the thick disk seems to be less extended, and does not appear as a distinct component between the thin disk and the halo. The vertical resolution of the observed distribution prevents any clear statement concerning the transition from the thin to thick disk, although it is apparent that the model is at variance with the data. This result raises the interesting question of the connections (or lack of) between the thin and thick disks. Almost since its discovery, it has been suggested that the thick disk is more akin to an extended thin disk (Norris 1987). Our knowledge of the thick disk more than twenty years later does not permit us to draw any firm conclusion on that point.

5 Conclusion

Investigation of the ([Fe/H], Z) distribution in the CFHTLS Wide fields does not seem to show a thick disc component as prominent and distinct as predicted by standard star-count models. The mean halo metallicity found to be –1.5 dex is in agreement with previous studies (e.g Bond et al. (2010), Sesar et al. (2011)). The behavior of models must be studied on more extensive data sets in order to assess the necessary adjustments and to better characterize the thick disk.

References

Arenou, F., Grenon, M., & Gomez, A. 1992, A&A, 258, 104
Bienayme, O., Robin, A. C., & Creze, M. 1987, A&A, 180, 94
Bond, N. A., Ivezić, Ž., Sesar, B., et al. 2010, ApJ, 716, 1

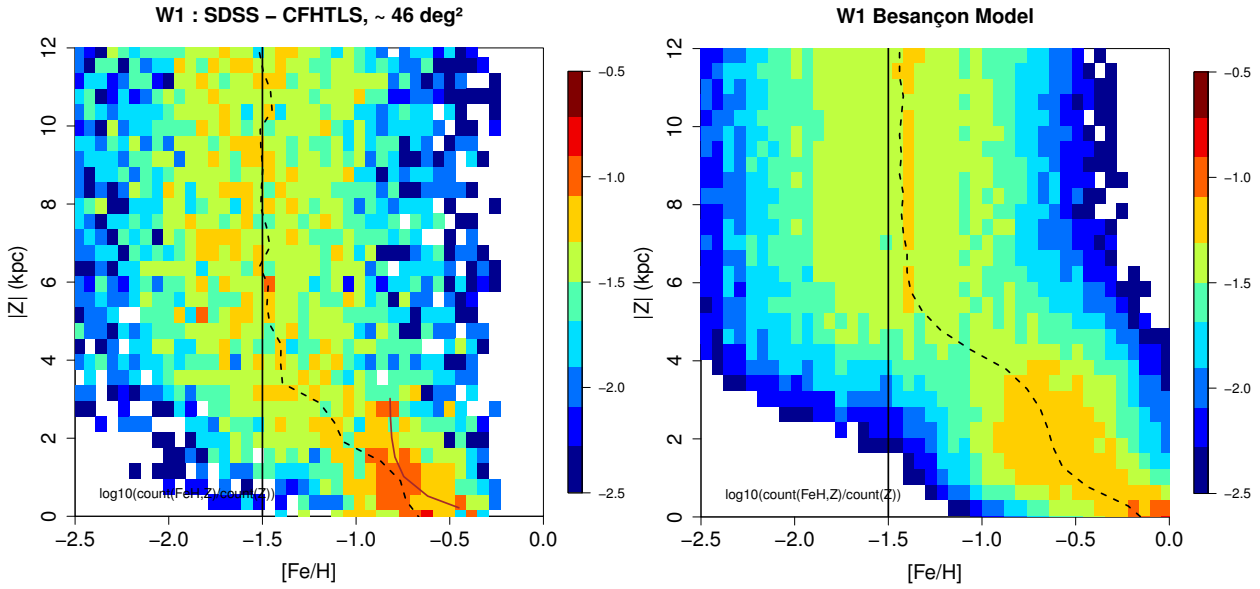

Fig. 2. Left: ([Fe/H], Z) distribution for CFHTLS/SDSS data in W1 field. **Right:** Besançon model ([Fe/H], Z) distribution in W1 field. The continuous line on the left plot shows the median metallicity formula (A2) derived by Bond et al. (2010). The dotted line represents the median metallicity per bin of 0.5 kpc.

Carollo, D., Beers, T. C., Chiba, M., et al. 2010, ApJ, 712, 692
de Jong, J. T. A., Yanny, B., Rix, H.-W., et al. 2010, ApJ, 714, 663
Hakkila, J., Myers, J. M., Stidham, B. J., & Hartmann, D. H. 1997, AJ, 114, 2043
Haywood, M., Robin, A. C., & Creze, M. 1997, A&A, 320, 428
Ivezić, Ž., Sesar, B., Jurić, M., et al. 2008, ApJ, 684, 287
Jones, D. O., West, A. A., & Foster, J. B. 2011, AJ, 142, 44
Jurić, M., Ivezić, Ž., Brooks, A., et al. 2008, ApJ, 673, 864
Lee, Y. S., Beers, T. C., An, D., et al. 2011, ApJ, 738, 187
Norris, J. 1987, ApJ, 314, L39
Robin, A. C., Reylé, C., Derrière, S., & Picaud, S. 2003, A&A, 409, 523
Schlegel, D. J., Finkbeiner, D. P., & Davis, M. 1998, ApJ, 500, 525
Sesar, B., Jurić, M., & Ivezić, Ž. 2011, ApJ, 731, 4